Journal of Bioscience and Bioengineering
VOL. 127 No. 3, 372–380, 2019

www.elsevier.com/locate/jbiosc

Role of cell-secreted extracellular matrix formation in aggregate formation and stability of human induced pluripotent stem cells in suspension culture

Mee-Hae Kim, Kazuhiro Takeuchi, and Masahiro Kino-oka*

Department of Biotechnology, Graduate School of Engineering, Osaka University, 2-1 Yamadaoka, Suita, Osaka 565-0871, Japan

Received 27 March 2018; accepted 23 August 2018
Available online 22 September 2018

Clinical and industrial applications require large quantities of human induced pluripotent stem cells (hiPSCs); however, little is known regarding the mechanisms governing aggregate formation and stability in suspension culture. To address this, we determined differences in growth processes among hiPSC lines in suspension culture. Using an hiPSC aggregate suspension culture system, hiPSCs from different lines formed multicellular aggregates classified as large compact or small loose based on their size and morphology. Time-lapse observation of the growth processes of two different hiPSC lines revealed that the balance between cell division and the extent of subsequent cell death determined the final size and morphology of aggregates. Comparison of the cell survival and death of two hiPSC lines showed that the formation of small, loose aggregates was due to continued cell death during the exponential phase of growth, with apoptotic cells extruded from growing hiPSC aggregates by the concerted contraction of their neighbors. Western blot and immunofluorescent staining revealed that aggregate morphology and proliferative ability relied to a considerable extent upon secretion of the extracellular matrix (ECM). hiPSCs forming large compact and stable aggregates showed enhanced production of collagen type I in suspension culture at 120 h. Furthermore, these aggregates exhibited higher expression of E-cadherin and proliferation marker Ki-67 as compared with levels observed in small and loose aggregates at 120 h. These findings indicated that differences in both aggregate formation and stability in suspension culture among hiPSC lines were caused by differences in ECM secretion capacity.

[**Key words:** Human induced pluripotent stem cells; Aggregate formation; Aggregate stability; Extracellular matrix; Suspension culture]

Human pluripotent stem cells (hPSCs), which include human embryonic stem cells and human induced pluripotent stem cells (hiPSCs), exhibit great potential as possible sources of cells for clinical and industrial applications due to their abilities to self-renew and differentiate into all cell types (1–3). These applications require large numbers of high-quality cells; however, the scalable production of hPSCs and their derivatives at a high density and under well-defined conditions remains challenging. To develop alternative cell-production strategies, a technique for hPSC expansion in three-dimensional (3D) suspension culture was recently established (4–11). The expansion of hPSCs has been demonstrated in dynamic suspension culture systems, followed by stirred-systems, such as spinner flasks and stirred-tank bioreactors (8–11). The 3D suspension culture of hPSCs results in aggregate formation, a process that can be controlled by several factors, including inoculation density, medium composition, and operation protocol (5,8,11). Although several types of hPSCs have demonstrated aggregate formation and stability, current approaches offer little control over parameters associated with the aggregation process (e.g., aggregate size, shape, and formation kinetics), thereby limiting optimization of cell expansion and differentiation processes and impeding identification of the requisite conditions for aggregate formation (4,6,11,12). There is growing interest in a better understanding of the mechanism of hPSC 3D aggregation, its impact on cell properties, and its feasibility in the design of culture processes.

The formation of 3D cellular aggregates is widely accepted as a dynamic process regulated by differential cellular adhesion, matrix synthesis, and remodeling (13–19). In contrast to two-dimensional (2D) culture systems, the formation of 3D aggregates in suspension culture is primarily mediated by cell-adhesion molecules, such as cadherin (20). After establishment of cell–cell interactions under physical forces or by spatial proximity, self-assembly of the 3D aggregate involves adapted cadherin interactions and/or the binding of integrin to extracellular matrix (ECM) proteins, enabling the formation of contacts between cells (20–22). The ECM is synthesized and secreted by cells beginning in the earliest stages of culture, and it provides structural and biochemical support to surrounding cells. During the early stage of aggregate formation, the cell-synthesized ECM (i.e., collagen type I) between cells is more diffuse, and cadherin-type cell–cell adherent junctions are the dominant forces behind initial aggregate formation. The ECM proteins produced in the aggregates not only function as signaling molecules in cell adhesion but also play a biomechanical role that influences the force balance and biomechanical signal transduction between the intracellular cytoskeleton and extracellular microenvironment (17,19). Therefore, changes in aggregate morphology could result from an active internal process, such as rearrangement of the cytoskeletal system. Additionally, ECM proteins play important roles in cell aggregation and influence aggregate stability and

* Corresponding author. Tel.: +81 6 6879 7444; fax: +81 6 6879 4246.
E-mail address: kino-oka@bio.eng.osaka-u.ac.jp (M. Kino-oka).

1389-1723/$ – see front matter
https://doi.org/10.1016/j.jbiosc.2018.08.010

compactness. There remain a number of unresolved questions regarding the key regulatory mechanisms governing aggregate formation and stability in dynamic suspension culture. Therefore, in this study, we investigated differences among hiPSC lines in their ability to form and maintain aggregates in suspension culture.

MATERIALS AND METHODS

hiPSC maintenance culture The hiPSC lines 1383D2 (provided by the Center for iPS Cell Research and Application, Kyoto University, Kyoto, Japan) (23) and Tic (JCRB1331; provided by the JCRB Cell Bank, Osaka, Japan) were routinely maintained on polystyrene substrate coated with recombinant laminin-511 E8 fragments (iMatrix-511; Nippi, Inc., Tokyo, Japan) in commercially available medium (StemFit AK02N; Ajinomoto Co., Inc., Tokyo, Japan). For subculture, single cells were seeded with 10 μM Rho-associated, coiled-coil containing protein kinase (ROCK) inhibitor (Y-27632; Wako Pure Chemical Industries, Osaka, Japan). The initial seeding was fixed at a viable cell density of 2.5×10^3 cells/cm^2, cells were incubated at 37°C in a humidified atmosphere with 5% CO_2, and medium was exchanged daily for fresh medium.

Static suspension culture For 3D suspension culture, cells were subcultured upon reaching 80%–90% confluence, as described previously (11,12). Briefly, hiPSCs were treated with 5 mM ethylenediaminetetraacetic acid/phosphate-buffered saline (PBS) with 10 μM ROCK inhibitor for 7 min at room temperature. Dissociation reagent (TrypLE Select; Invitrogen, Carlsbad, CA, USA) with 10 μM ROCK inhibitor was then applied for another 7 min at room temperature. After centrifugation, single hiPSCs were re-suspended in fresh medium. Viable cells were counted with a cell counter (TC20; Bio-Rad, Hercules, CA, USA) using the trypan blue exclusion method. After dissociating hiPSCs into single cells by pipetting, cells were cultured on 3D culture plates with micro-spaces on the surface (Elplasia; Kuraray Co., Ltd., Tokyo, Japan). The hiPSCs in fresh medium with a ROCK inhibitor were seeded with 2 mL of cell suspension at a concentration of 2.5×10^5 cells/mL/well in order to produce uniform aggregates (200 cells/aggregate). Beginning on the day following aggregate formation, the medium was exchanged for fresh medium every 24 h. Experiments were performed in the presence and absence of 10 μM ROCK inhibitor, which was added during the first 24 h when used.

Time-lapse live-cell imaging To monitor the aggregate-growth processes of hiPSCs in suspension culture, we used a phase-contrast time-lapse observation incubator (BioStudio-T; Nikon Engineering, Kanagawa, Japan) equipped with a camera for video imaging. Cultures were observed through a 4× objective lens, and images were obtained every hour at several positions.

To understand the cell-growth-phase-dependent induction of cell survival or death within the aggregates, viability was determined using the EasyProbes cell viability imaging kit (Applied BioProbes, Eugene, OR, USA). Briefly, 2.5×10^5 cells/mL per well were loaded into 3D culture plates with a glass bottom for high-quality imaging (Elplasia; Kuraray Co., Ltd.) on experimental day 2 after aggregate formation. The nuclei of both live and dead cells were then stained according to manufacturer protocol, and images were acquired by confocal laser scanning microscopy (model FV-10i; Olympus, Tokyo, Japan) with a 60× objective lens under a fluorescence channel (excitation at 488 and 594 nm) and a phase-contrast channel.

Preparation and staining of frozen sections The procedure used for immunofluorescent staining of cryostat sections was similar to that described previously (11,24). Briefly, hiPSC aggregates were fixed with 4% paraformaldehyde (Wako Pure Chemical Industries) for 10 min at room temperature and then rinsed with PBS. After fixation, 3D aggregates were transferred to embedding medium (OCT, Tissue-Tek; Sakura Fine Technical, Tokyo, Japan) and quickly frozen in liquid nitrogen. Cells were cut into 10-μm thick sections using a cryostat (Leica CM1850; Leica, Wetzlar, Germany) and thaw-mounted onto the pre-coated slides, after which they were soaked for 4 min in PBS containing 0.25% Triton X-100. After masking nonspecific proteins via incubation in Block Ace (Dainippon Sumitomo Pharma Co., Ltd., Osaka, Japan) for 1 h at ambient temperature, cells were incubated with the following primary antibodies (diluted adequately in PBS containing 10% Block Ace) at 4°C overnight: anti-collagen I (Abcam, Cambridge, MA, USA), anti-fibronectin (Santa Cruz Biotechnology, Dallas, TX, USA), anti-laminin α5 (Abcam), anti-E-cadherin (Santa Cruz Biotechnology), anti-cleaved caspase-3 (Cell Signaling Technology, Beverly, MA, USA), and anti-Ki67 (Santa Cruz Biotechnology). Cells were washed with Tris-buffered saline (TBS) and immunolabeled with Alexa Fluor 488-conjugated goat anti-rabbit or Alexa Fluor 594-conjugated goat anti-mouse IgG (Life Technologies, Grand Island, NY, USA) for 1 h. Cell nuclei were stained with 4′,6-diamidino-2-phenylindole (DAPI; Life Technologies), and images were obtained using a confocal laser scanning microscope (model FV-1000; Olympus) with a 60× objective lens and an image analyzer or a 10× objective lens under fluorescence excitation at 358 nm, 488 nm, and 594 nm.

Protein extraction and western blot analysis Protein extraction and western blot analysis were conducted using methods similar to those described previously (25). Total cellular protein was extracted from cells using CelLytic mammalian cell lysis/extraction reagent (Sigma–Aldrich, St. Louis, MO, USA). Total protein in conditioned medium was precipitated with trichloroacetic acid at 4°C for 30 min, and equal quantities of protein lysates were separated by sodium dodecyl sulfate polyacrylamide gel electrophoresis and transferred to nitrocellulose membranes using standard methods. Blots were blocked in 5% nonfat dry milk in TBS (pH 7.4) before incubation with primary antibodies in 5% milk/TBS. Blots were rinsed three times and washed four times for 5 min each in TBS + 0.1% Tween 20. Membranes were blocked in PBS containing 5% milk powder and 0.05% Tween 20 for 1 h at room temperature and incubated overnight at 4°C with the anti-collagen I antibody (Abcam). After washing and 1 h of incubation at room temperature with horseradish peroxidase-conjugated goat anti-rabbit IgG secondary antibody, immunoreactive proteins were detected with an enhanced chemiluminescence system (Amersham Bioscience, Piscataway, NJ, USA). β-Actin was used as a loading control.

Flow cytometry To analyze the expression of surface markers by flow cytometry, hiPSCs were harvested and processed as described previously (11). Cells were treated with the Cytofix/Cytoperm permeabilization kit (BD Biosciences, San Jose, CA, USA) and incubated with primary antibody [mouse monoclonal octamer-binding transcription factor (OCT)3/4; Santa Cruz Biotechnology] and secondary antibody (allophycocyanin-conjugated anti-mouse IgG; BD Biosciences). Direct staining of stage-specific embryonic antigen 4 (SSEA4) was performed using human/mouse SSEA4 fluorescein (R&D Systems, Minneapolis, MN, USA). Flow cytometry was performed with a flow cytometer (Sysmex Corporation, Kobe, Japan), and data were analyzed with commercially available software (FlowLogic, Inivai Technologies, Mentone, Victoria, Australia).

Quantitative real-time RT-PCR RNA isolation, cDNA synthesis, and quantitative real-time RT-PCR (qRT-PCR) assays were carried out as described previously (25). Total RNA was extracted from the cells (RNeasy mini kit; Qiagen, Hilden, Germany) according to manufacturer instructions. Reverse transcription was conducted using a SuperScript II reverse transcriptase kit (Takara Bio, Shiga, Japan), and real-time PCR was performed using SYBR Premix EX Taq (Takara) on a 7300 real-time PCR system (Applied Biosystems, Foster City, CA, USA). Relative gene expression was normalized to glyceraldehyde-3-phosphate dehydrogenase (GAPDH) expression in order to obtain the ΔC_t value. All PCR products were evaluated according to melting curve analysis in order to exclude the possibility of multiple products or incorrect product size. The primer sequences are provided in Table S1.

Statistical analysis All experiments were repeated at least three times to ensure reproducibility. Data were analyzed for statistical significance using Student's t tests, and a $p < 0.05$ was considered statistically significant.

RESULTS

Differences in morphological and growth characteristics among hiPSC lines in suspension culture To investigate the ability of hiPSC sources to readily aggregate, we cultured two lines of hiPSCs (1383D2 and Tic) for several passages prior to aggregation in a 2D maintenance culture system using a single-cell-passaging method. Both cell lines grew well in monolayer culture and exhibited similar compact colony morphologies. Flow cytometry analysis showed that 91%–99% of the cells were positive for stem cell markers, such as OCT3/4 and SSEA4 (Fig. S1).

To better understand the initiation and progression of aggregate formation in two different hiPSC lines in suspension, cells were dissociated into single cells and seeded at a concentration of 1×10^5 cells/mL/well into a micro-space cell-culture plate. A high percentage of the aggregates within each micro-space in the cell-culture plate were filled, and the formation of aggregates from single cells was relatively uniform in size and shape, similar to previously published reports (4). Each hiPSC lines were observed to generate uniform, round aggregates with distinct morphologies, indicating that independent hiPSC lines appeared to exhibit noticeable effects on aggregate size and morphology at 120 h. Fig. 1 shows the morphological differences between aggregates from the two different hiPSC lines. We classified the cell lines into two distinct morphological groups, referred to as large compact and small loose aggregates. All cells observed in suspension culture were found to possess aggregation potential; however, there were significant differences in the aggregation and proliferative capacities of the two hiPSC lines based on the presence or absence of ROCK inhibitor (10 μM) during the first 24 h. The dissociated 1383D2 cells spontaneously formed aggregates within 24 h and exhibited proliferative growth by 24 h without the need for the

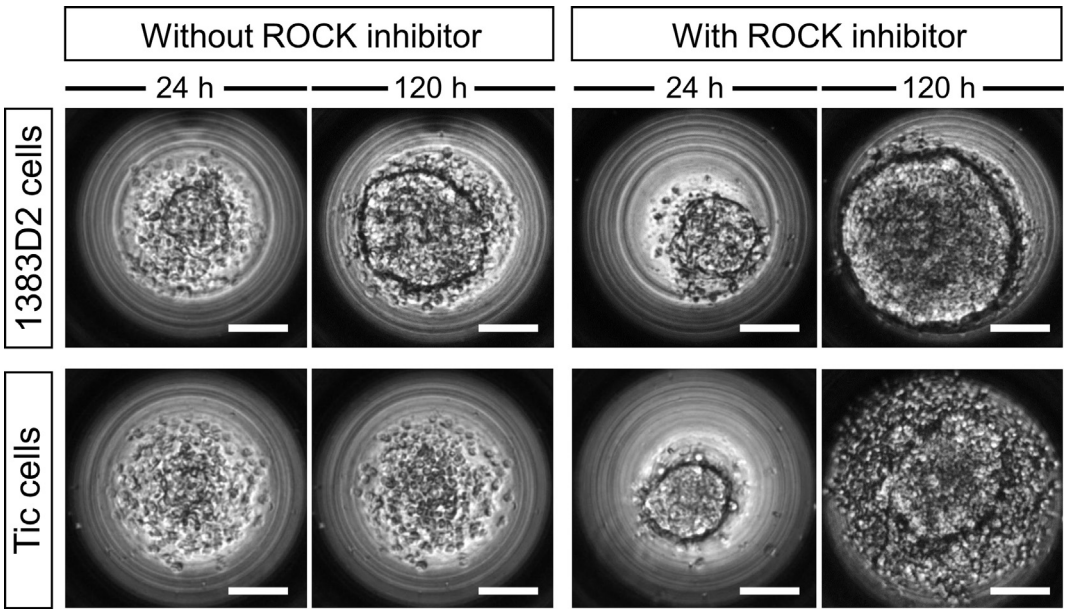

FIG. 1. Morphological characterization and growth patterns of two different hiPSC lines (1383D2 and Tic) in suspension culture with or without ROCK inhibitor. ROCK inhibitor was added to the cultures for the first 24 h to prevent apoptosis after single-cell dissociation. Scale bars: 100 μm. See Supplementary Movie S1.

ROCK inhibitor (Movie S1). These aggregates progressively increased in size and then appeared as compact aggregates after 120 h. By contrast, the dissociated Tic cells died, and no cell aggregates were formed, emphasizing the need for the ROCK inhibitor to initiate cell growth. When the ROCK inhibitor was added to the suspension cultures, both hiPSC lines exhibited potentiated survival following single-cell dissociation, and aggregates formed within 24 h. However, the aggregates formed from these two hiPSC lines displayed distinct behaviors in the growth phase, followed by culture under regular growth conditions for the next 94 h. Although 1383D2 cells formed compact aggregates with smooth surfaces in which individual cells could not be distinguished, Tic cells formed only loose cellular aggregates in which individual cells remained clearly identifiable. Therefore, Tic cells formed small loose aggregates with a rough surface. After suspension culture for 120 h, the average aggregate sizes of 1383D2 and Tic cells were ~310 μm and ~210 μm, respectively, with >92% of the cells positive for OCT3/4 according to flow cytometric analysis and exhibiting expression levels similar to those found in cells grown under 2D monolayer culture (Fig. S2).

Supplementary video related to this article can be found at https://doi.org/10.1016/j.jbiosc.2018.08.010.

Extended observations by fluorescence microscopy allowed observation of differential distributions of live and dead cells within the aggregates. Cells within aggregates actively divided, but cell death continued after division. Moreover, cells surrounding apoptotic cells selected for extrusion collectively crawled towards the outside of the aggregate (Fig. 2 and Movie S2). This action levered the apoptotic cells out of the aggregates, causing their extrusion. Comparison of cell viability between the two hiPSC lines revealed that the large compact aggregates of 1383D2 cells contained fewer apoptotic cells than the small loose aggregates of Tic

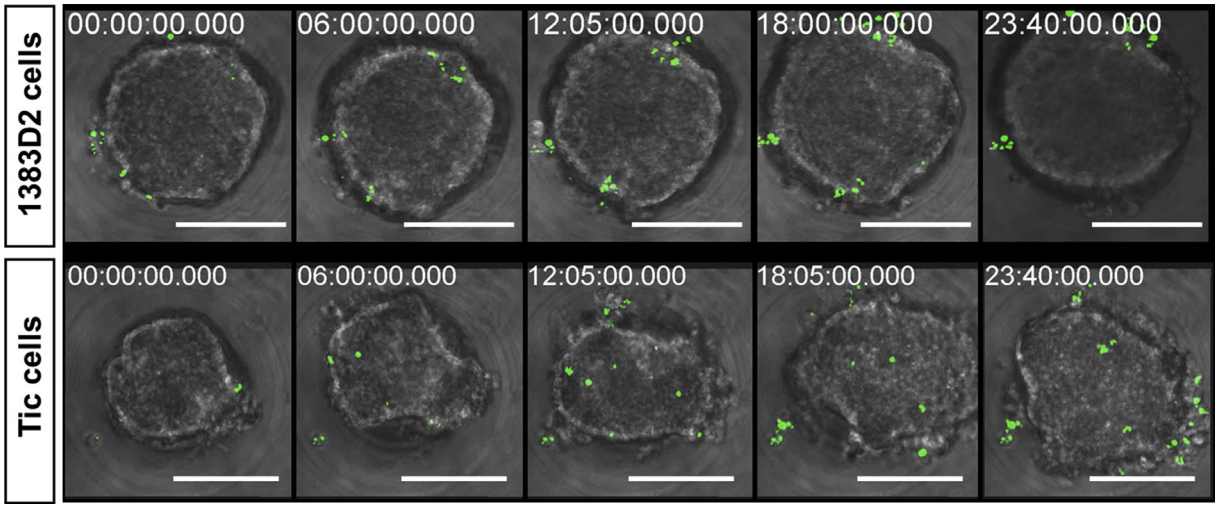

FIG. 2. Fluorescent images of dead cells and phase-contrast images showing growing aggregates of two different hiPSC lines (1383D2 and Tic). Cells were grown in medium supplemented with ROCK inhibitor for the first 24 h after inoculation, and the stained nuclei of both live and dead cells were observed at between 48 h and 72 h of suspension culture. The green fluorescent signal corresponds to dead cells. Scale bars: 100 μm. See Supplementary Movie S2.

cells. In the large compact aggregates of 1383D2 cells, cell death occurred at the aggregate periphery, whereas in the small loose aggregates of Tic cells, dead cells were prominently distributed throughout the aggregate. These apoptotic cells were efficiently removed by neighboring cells, and were, therefore, mostly found at the outermost edges of the aggregates.

Supplementary video related to this article can be found at https://doi.org/10.1016/j.jbiosc.2018.08.010.

Characterization of gene-expression patterns among hiPSCs in suspension culture To evaluate gene expression caused by growth differences between hiPSC lines in suspension culture, we analyzed caspase-3 (an apoptosis-related gene) and survivin (an anti-apoptotic gene). Caspase-3 expression gradually decreased over time, whereas the survivin expression increased over time (Fig. S3). At 24 h, survivin exhibited higher expression, and caspase-3 exhibited lower expression in large compact aggregates of 1383D2 cells as compared with their levels in small loose aggregates of Tic cells. When comparing expression differences between hiPSC lines at the end of culture of 120 h, survivin expression in large compact aggregates of 1383D2 cells was 1.3-fold higher than that in small loose aggregates of Tic cells; however, no significant differences were observed between the expression levels of caspase-3 in the two hiPSC lines.

To determine whether the expression pattern of apoptosis-related genes was similar to or different from that of cell-adhesion molecules and ECM-related components, we assessed the expression of two cell-adhesion molecules (E-cadherin and integrin β1) and three ECM-component transcripts [collagen type I (COL1A1), fibronectin (FN1), and laminin (LAMA5)]. E-cadherin and integrin β1 expression was observed in 1383D2 cells within 24 h of culture, followed by a period of steady expression that continued for 120 h, whereas their expression in Tic cells was significantly higher at all time points relative to 1383D2 cells, although their levels did not change significantly over time. A different expression pattern of ECM components was observed between hiPSC lines. In 1383D2 cells forming large compact aggregates, COL1A1 expression increased significantly by 24 h and gradually increased over time, with COL1A1 expression 1383D2 cells 1.2-fold higher than that in Tic cells at 120 h. By contrast, FN1 expression increased significantly in Tic cells over time and was 1.4-fold higher than that in 1383D2 cells at 120 h. However, no significant differences were observed in LAMA5 expression between the two hiPSC lines by 72 h, although its expression changed significantly at 120 h.

Spatiotemporal localization of ECM components and E-cadherin within hiPSC aggregates To gain insight into the differential behaviors of hiPSC lines with respect to aggregate formation, we prepared histological sections of aggregates. We investigated the ECM components produced by the cells forming the aggregates in order to evaluate correlations between aggregate formation and ECM production in cultures treated with ROCK inhibitor for the first 24 h. The expression and presence of collagen I, fibronectin, and laminin α5 in aggregates were assessed by immunostaining and western blot analysis at the culture endpoint (120 h). In 1383D2 cells, which form large compact aggregates, two distinct areas were identified within the stained sections. Cells in the outer layer were more tightly packed than those within the core (Fig. 3). Consequently, the cell nuclei in the core were more spherical than those at the outer edge, and we observed a

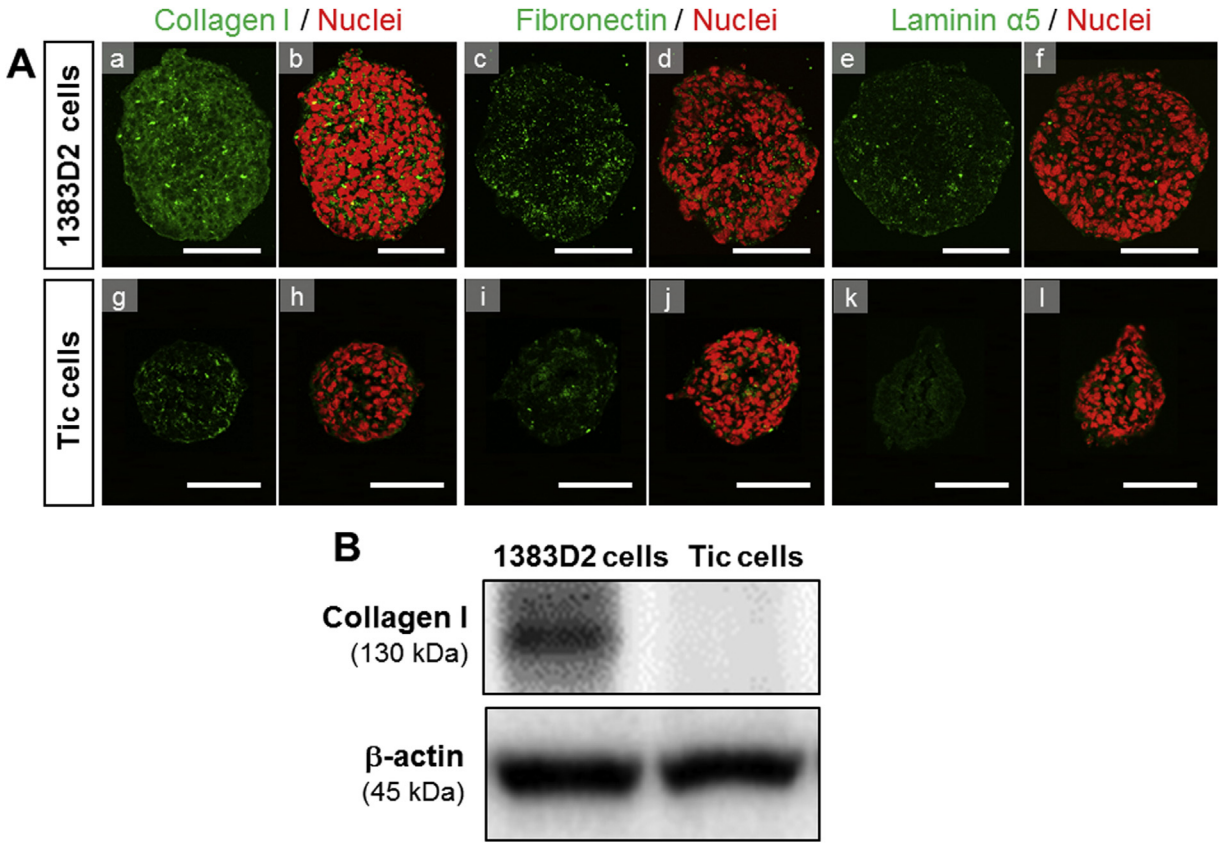

FIG. 3. Characterization of ECM production in aggregates of two different hiPSC lines (1383D2 and Tic) cultured in suspension. Cells were grown in medium supplemented with ROCK inhibitor for the first 24 h after inoculation. (A) Representative immunofluorescence staining of hiPSC aggregate structures of 1383D2 (a–f) and Tic (g–l) cells after growth for 120 h in suspension culture using antibodies against collagen I, fibronectin, and laminin α5. Cell nuclei were stained with DAPI (red). Scale bars: 100 μm. (B) Western blot of collagen I in two hiPSC lines in static suspension culture at 120 h.

uniform distribution of fibronectin and laminin α5 expression, with interspersed regions of collagen I deposition throughout the compact aggregates. Compared with expression levels in 1383D2 cells, all ECM components were weakly expressed in Tic cells. In particular, collagen I was more highly expressed in 1383D2 cells forming compact aggregates than in those forming loose aggregates. These findings indicated that hiPSCs forming large compact aggregates exhibited a greater capacity to secrete collagen I in suspension culture.

Subsequently, immunostaining for E-cadherin and collagen I showed notable differences in their expression patterns that were hiPSC-line-dependent. In 1383D2 cells, which form large compact aggregates, E-cadherin was expressed by densely packed cells in the center of the aggregate at an early time point (24 h), and its expression continued to increase until the end of culture (120 h) (Fig. 4). Similarly, collagen I was expressed in the central regions of the aggregates at 24 h, and strong staining was detected throughout the aggregate at 120 h. When E-cadherin localization was compared with that of collagen I inside of these aggregates, E-cadherin was predominantly expressed in all cells and could be observed as a continuous line present at the boundaries between neighboring cells throughout the entire aggregate. The distribution of collagen I in the aggregate was similar to the positive distribution represented by E-cadherin staining. By contrast, the small loose aggregates of Tic cells exhibited weaker collagen I and E-cadherin expression throughout the aggregate during culture.

Spatiotemporal localization of Ki-67 and cleaved caspase-3 within hiPSC aggregates To assess the consequences of hiPSC aggregate formation, we used immunostaining to determine the expression of Ki-67 (a marker of proliferation) and cleaved caspase-3 (an apoptotic cell marker). In 1383D2 cells forming large compact aggregates, Ki-67 was detected throughout the cell aggregates at 24 h, and fluorescence was markedly increased at 120 h (Fig. 5). There were very few cleaved caspase 3-positive cells in the peripheral region at 24 h, with these almost completely disappearing at 120 h. Comparison of the central and peripheral regions of the loose aggregates of Tic cells revealed that Ki-67-positive cells were only detected in densely packed cells in the center of the aggregate, whereas cleaved caspase-3 appeared randomly distributed throughout the aggregate, with no clustering in specific areas. These results indicated the presence

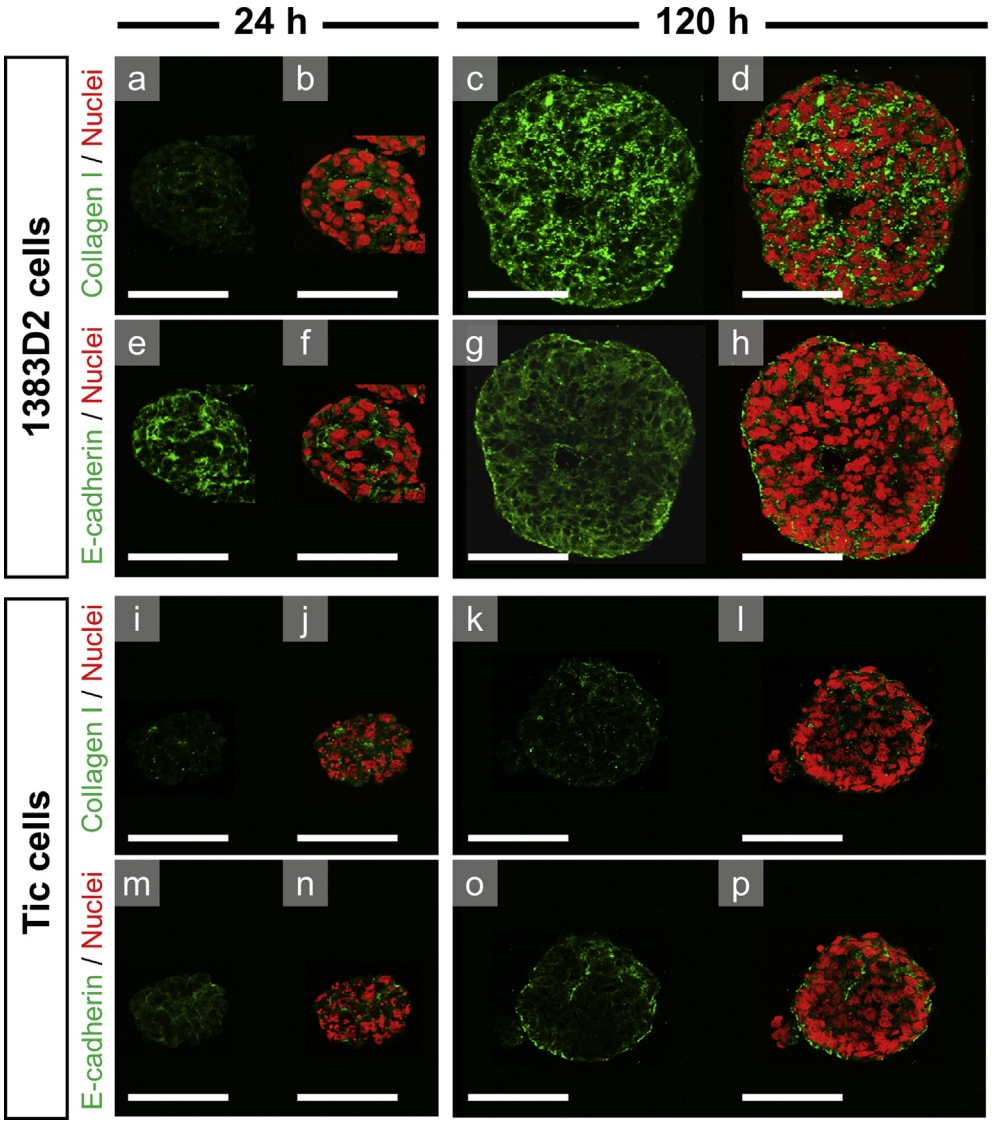

FIG. 4. Localization of collagen I and E-cadherin in aggregates from two different hiPSC lines (1383D2 and Tic) in suspension cultures. Cells were grown in medium supplemented with ROCK-inhibitor for the first 24 h after inoculation. Cryosections of hiPSC aggregates of 1383D2 (a–h) and Tic (i–p) cells were immunostained with E-cadherin (green) and collagen I (green). Cell nuclei were stained with DAPI (red). Scale bars: 100 μm.

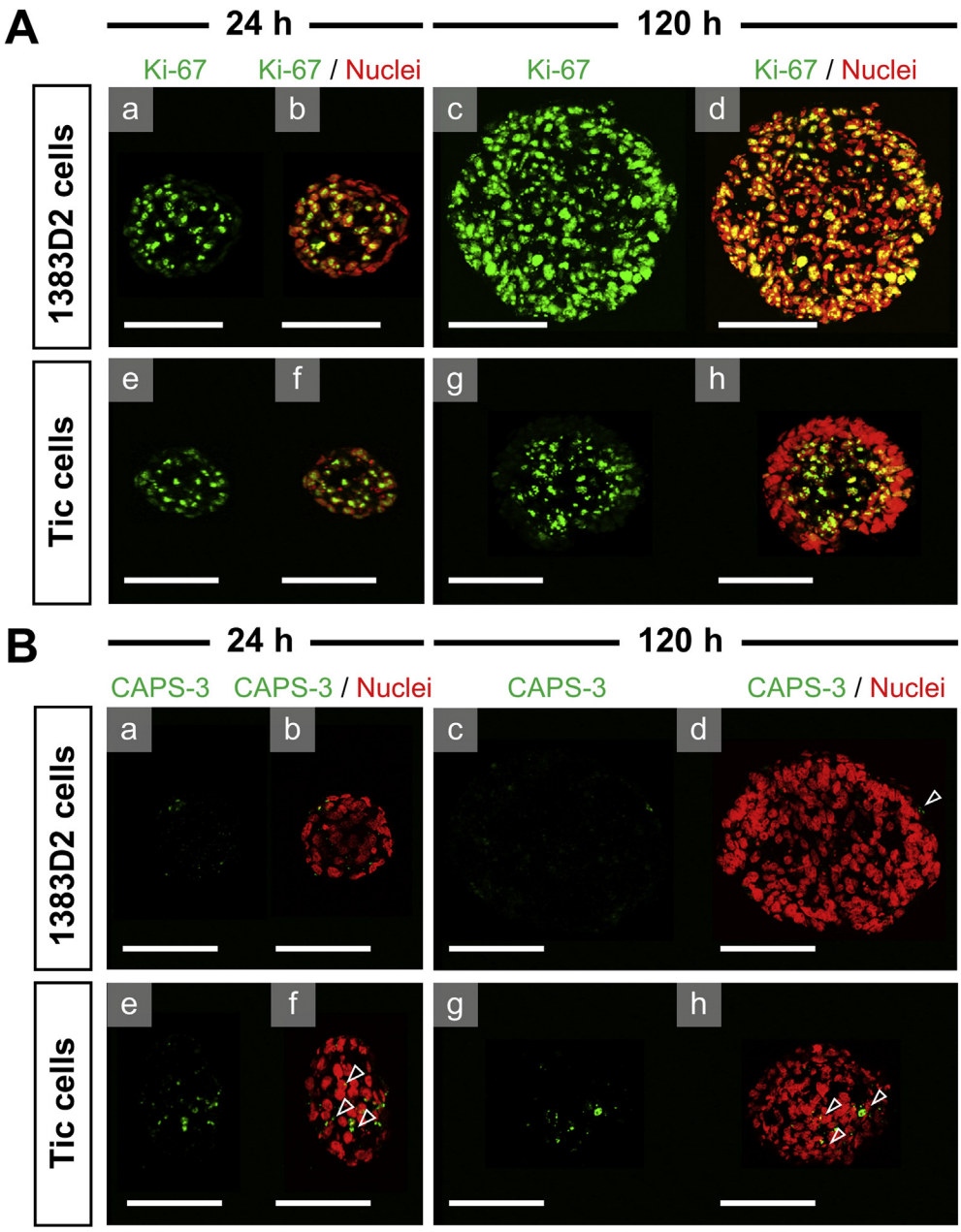

FIG. 5. Localization of Ki-67 and cleaved caspase-3 (CAPS-3) in aggregates from two different hiPSC lines (1383D2 and Tic) in suspension cultures. Cells were grown in medium supplemented with ROCK inhibitor for the first 24 h after inoculation. (A) Immunofluorescence staining of Ki-67 (green) in hiPSC aggregate cryosections of 1383D2 (a–d) and Tic (e–h) cells at 24 h and 120 h. Cell nuclei were stained with DAPI (red). (B) Immunofluorescence staining of cleaved caspase-3 (green) in hiPSC aggregate cryosections 1383D2 (a–d) and Tic (e–h) cells at 24 h and 120 h. Cell nuclei were stained with DAPI (red). Arrows indicate cleaved caspase-3-positive cells. Scale bars: 100 μm.

of spatial and temporal differences in the localization of cell proliferation and apoptosis between different types of hiPSC aggregates in suspension culture.

DISCUSSION

A key aspect of the scaling-up of an aggregate-based culture system is the formation and stability of the aggregates. Many investigators noted fluctuations in aggregate magnitude and frequency in 3D suspension culture, and aggregate characteristics are dependent upon the cell line being used, as well as the composition of the medium and agitation rate, the latter of which plays the most important role in aggregation size (4,11,12). We previously described significant differences in aggregate morphology and growth capacity among hiPSC lines in 3D suspension culture, even when inter-line differences in 2D culture were not significant. A crucial question in this context is why only certain cell lines appear to aggregate readily in suspension culture, whereas others do not. To elucidate the mechanism underlying the initiation and progression of aggregate formation, we clarified whether the capacity to form cell–cell interactions affected the extent of cell aggregation in the absence of ROCK inhibitor and, if so, to study the differences between hiPSC lines in terms of aggregate formation and stability separate from the effects of the ROCK inhibitor. When cultured in suspension, hiPSCs from different lines formed multicellular

aggregates that could be classified as large compact or small loose aggregates based on the size and morphology of the aggregates. Although no difference in the initiation of aggregate formation was observed between the lines when ROCK inhibitor was present for the first 24 h, different capacities for aggregation were observed in the absence of ROCK inhibitor. The two hiPSC lines exhibited different capacities for aggregate formation, with 1383D2 cells forming large compact aggregates and Tic cells forming small loose aggregates that did not undergo compaction (Fig. 1 and Movie S1). Dissociated 1383D2 cells spontaneously formed aggregates within 24 h and exhibited proliferative growth by 24 h without the need for the addition of ROCK inhibitor. By contrast, dissociated Tic cells died, and no cell aggregates were formed, emphasizing the need for the addition of ROCK inhibitor for the initiation of cell growth. This indicated that differences between cell lines in cell-aggregation capacity in suspension affected certain aspects of cell viability. The phenomenon of aggregate formation comprises mechanical stretching and compression between adjacent cells and requires active contraction of the actin cytoskeleton tethered to intercellular cadherin contacts (18,26). Cell–cell contact mediated by cadherins provides an escape pathway for the avoidance of apoptosis and secondarily facilitates cell growth in the absence of integrin-generated signals in suspension culture (19,21). These findings indicate that cell-aggregation capacity associated with E-cadherin-mediated cell–cell contacts in single-cell suspension enhances the capacity for building an ECM environment within the aggregate.

Furthermore, we clarified whether cell-secreted ECM affected the survival and proliferative ability of hiPSCs in the presence of ROCK inhibitor. Comparison of cell survival and death between the two hiPSC lines showed that the small loose aggregates resulted from continued cell death during the growth phase, with apoptotic cells extruded from the growing aggregate by the concerted contraction of their neighbors (Fig. 2 and Movie S2). This process involves a novel mechanism in which apoptotic cells signal their immediate neighbors to reorganize their actin cytoskeleton and actively extrude the dying cells (26). By removing the dying cells and repairing the resulting gaps, the extrusion process maintains the size and morphology of the aggregates. Additionally, the location of proliferating cells within an aggregate mainly differs with regard to ECM location. Previous studies reported that collagen I plays a fundamental role in cell adhesion and aggregate formation in hiPSC suspension culture (4,11). In the present study, we demonstrated a strong positive correlation between collagen I expression and that of Ki-67 in hiPSC suspension culture. In 1383D2 cells, which formed large compact aggregates, collagen I was expressed by cells in the central regions throughout the aggregates at an early time point (24 h) and was highly expressed throughout the aggregate at the end of the culture period (120 h) (Fig. 3). The distributions of collagen I and Ki-67 in the aggregates were similar to that of E-cadherin (Figs. 4 and 5). However, in Tic cells forming loose aggregates that did not undergo compaction, the small number of cells expressing Ki-67 in the central regions of the

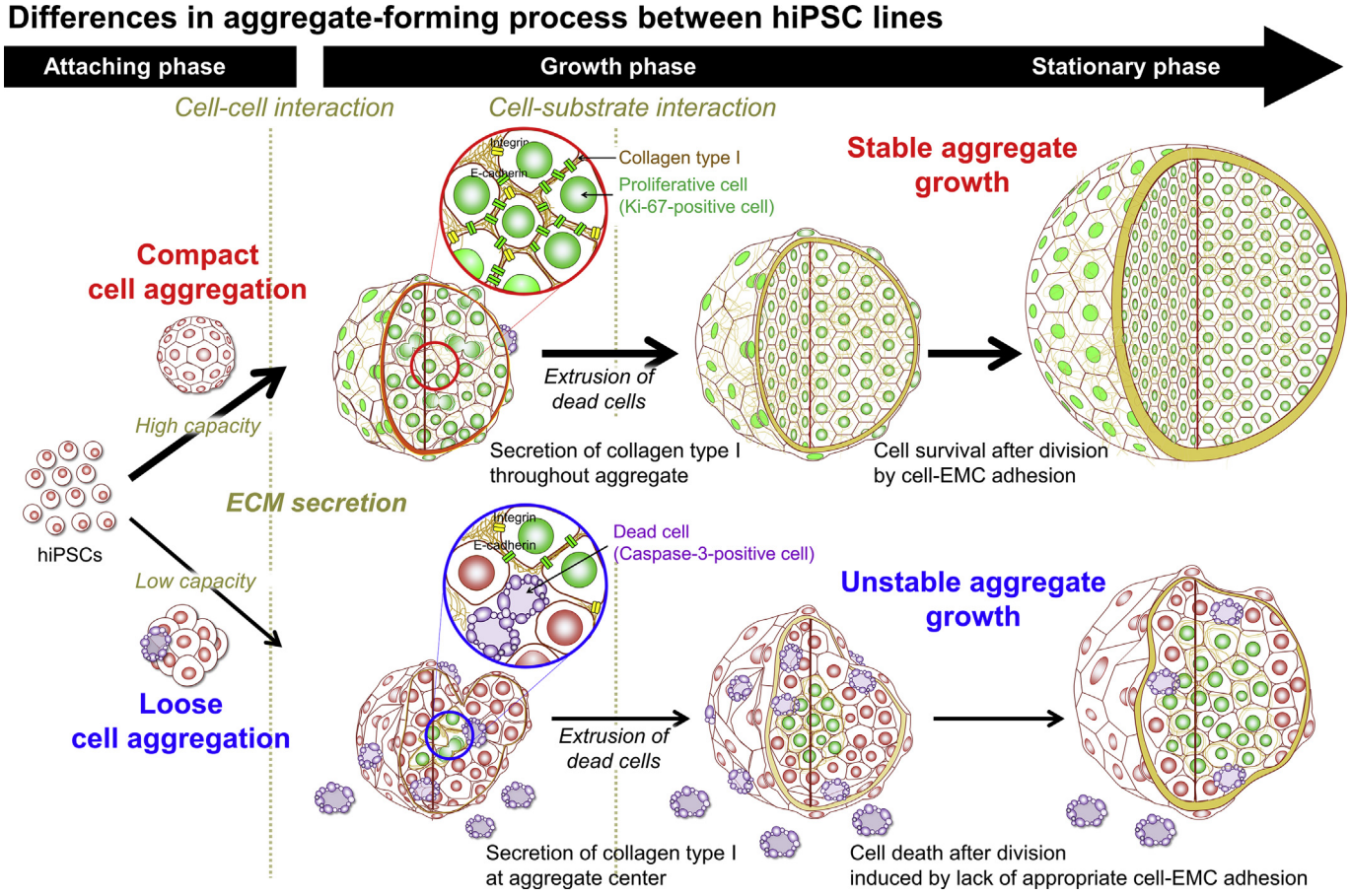

FIG. 6. Schematic showing the proposed mechanism by which cell-derived ECM acts as a key regulator of aggregate formation and stability in single-cell-inoculated suspension culture. Two hiPSC lines showed distinct morphologies and growth characteristics, indicating that ROCK inhibitor is important for the survival of the initial single hiPSCs and growth after forming hiPSC aggregates. The upper images show the sequence of events leading to aggregate formation in static and dynamic suspension culture. Survival and proliferation of hiPSCs can be achieved by utilizing either the cell–ECM-interaction-mediated integrin pathway or the cell–cell interaction-mediated E-cadherin pathway. This suggests that (i) cell-derived ECM enhances cell viability and aggregate growth, consequently resulting in increased cell survival, and (ii) the capacity for ECM production of single hiPSCs is generally supported by treatment with ROCK inhibitor, ultimately resulting in cell expansion in suspension culture.

aggregates led us to conclude that ECM-secreting cells exhibit higher proliferative capacity. These observations indicated that differences in shape and the internal arrangement of cells between the two types of aggregates stem from differences in the expression of ECM components, with cells forming more extended contacts ultimately being deformed by them and consequently resulting in their aggregates becoming more compact. This hypothesis suggests that the capacity to form cell–cell interactions leads to differences in the extent of cell aggregation, as well as aggregate formation and stability.

Here, we propose a model for the mechanism underlying the differences among hiPSC lines in suspension culture based on the results obtained in this study and in previous studies (Fig. 6). Two main conclusions can be drawn from our results. First, when hiPSCs are grown in suspension culture, cells spontaneously undergo aggregate formation or cell death. Second, a greater capacity for cells to aggregate promotes cell survival and proliferative ability. This leads to the question of whether a relationship exists between reduced cell–cell adhesion after cell dissociation and the capacity of the cell to secrete the ECM components necessary for the formation of cell–substrate adhesions. The process of hPSC aggregate formation, typically via the self-aggregation of singularized cells, is a critical initial step for cell growth in suspension culture (26–29). Cell–cell and cell–substrate interactions regulate Rho family signaling, and enzyme treatment induces irreversible cell–cell and cell–substrate interactions in hPSCs. As a result, dissociating hPSCs into single cells leads to Abr-dependent RhoA and ROCK activation, followed by downstream actomyosin hyperactivation and apoptosis (30). Several studies revealed that cell survival depends upon a constant supply of survival signals provided by neighboring cells and the ECM (26,28). The ECM plays a role in the complex interplay of growth-regulatory pathways, for example by promoting survival and proliferation in suspension cultures of hPSCs, which is mediated through the phosphoinositide 3-kinase/AKT pathway (31). Furthermore, cell–cell interactions are made through integrin–ECM bridges or cadherin-mediated interactions depending on the cell type, with the subsequent cell-mediated contractility producing compact 3D aggregates (14,15). Once aggregates have formed, the ECM-secreting and -remodeling activities of hiPSCs are necessary to maintain cohesion (18). The compressive strength and size of an aggregate gradually increase over time due to the cell-derived ECM, although it appears that cells lose their capacity to interact with surrounding collagen fibers, thereby losing the traction forces necessary to change shape (19). These results suggest that the phenotypic differences among various hiPSC lines are related to the ECM-secreting capacity in the resulting hiPSCs, which continues to affect cell survival and growth capacity. These differences might stem from differences in the relative adhesiveness of different cell types for each other or in the ability and kinetics of ECM production, which helps stabilize the aggregates after their initial formation. The balance between cell division and subsequent cell death determines the final size and morphology of the aggregates. It is likely that the capacity of hPSCs to secrete ECM proteins prevents cell death via apoptosis due to the lack of integrin-mediated survival signals, thereby promoting their survival (30,31). The different morphologies of the aggregates can be attributed to the ECM, which is involved in regulating the shape and movement of cells by acting on stress fibers. These differences might be due to changes in matrix stiffness or porosity that are transduced into the cells via integrin and focal-adhesion signaling, consequently affecting processes, such as signaling responses and gene expression (19,21). Our comparison of the aggregate-formation process in different hiPSC lines and culture conditions supports the view that ECM secretion faithfully enhances cell survival and stable aggregate formation and establishes an aggregate that is robust to cell expansion in suspension culture. Therefore, our results provide insight into the variability observed between cell lines and enable general conclusions regarding the functional similarities between hiPSC lines in suspension culture.

In conclusion, we demonstrated that the cell-secreted ECM plays a key role in cell aggregation, spherical aggregate formation, and cohesion in suspension culture systems. Differences in cell-aggregation capacity and ECM secretory capacity exist between hiPSC lines and lead to important differences in the initiation and progression of aggregate formation. For generating large compact aggregates, the cell-adhesive capacity and ECM-secreting and -remodeling activities of hiPSCs in suspension culture are necessary and undergo further upregulation upon aggregate formation and survival in suspension culture. Therefore, an understanding of the major differences between hiPSC lines in terms of aggregate formation and stability is essential to ensure optimal growth in suspension culture. We anticipate that approaches using cell-derived ECM will fuel the development of 3D cellular constructs, ultimately leading to large-scale expansion culture processes.

Supplementary data related to this article can be found at https://doi.org/10.1016/j.jbiosc.2018.08.010.

ACKNOWLEDGMENTS

We are grateful to Mr. G. Kobayashi and Mr. S. Ayanao (Kuraray Co., Ltd., Tokyo, Japan) for their preparation and characterization of the micro-spaces cell-culture plate. This work was supported by the project “Development of cell manufacturing and processing system for industrialization of regenerative medicine” (No. P14006) commissioned by the Japan Agency for Medical Research and Development, Japan. This work also was supported by a joint research project with Institute for Innovation, Ajinomoto Co., Inc., Japan.

References

1. **Kimbrel, E. A. and Lanza, R.:** Current status of pluripotent stem cells: moving the first therapies to the clinic, Nat. Rev. Drug Discov., **14**, 681–692 (2015).
2. **Okita, K. and Yamanaka, S.:** Present and future challenges of induced pluripotent stem cells, Philos. Trans. R. Soc. Lond. B Biol. Sci., **370**, 20140367 (2015).
3. **Osafune, K., Caron, L., Borowiak, M., Martinez, R. J., Fitz-Gerald, C. S., Sato, Y., Cowan, C. A., Chien, K. R., and Melton, D. A.:** Marked differences in differentiation propensity among human embryonic stem cell lines, Nat. Biotechnol., **26**, 313–315 (2008).
4. **Kato, Y., Kim, M.-H., and Kino-oka, M.:** Comparison of growth kinetics between static and dynamic cultures of human induced pluripotent stem cells, J. Biosci. Bioeng., **125**, 736–740 (2018).
5. **Bratt-Leal, A. M., Carpenedo, R. L., Ungrin, M. D., Zandstra, P. W., and Mcdevitt, T. C.:** Incorporation of biomaterials in multicellular aggregates modulates pluripotent stem cell differentiation, Biomaterials, **32**, 48–56 (2011).
6. **Nie, Y., Walsh, P., Clarke, D. L., Rowley, J. A., and Fellner, T.:** Scalable passaging of adherent human pluripotent stem cells, PLoS One, **9**, e88012 (2014).
7. **Dang, S. M., Gerecht-Nir, S., Chen, J., Itskovitz-Eldor, J., and Zandstra, P. W.:** Controlled, scalable embryonic stem cell differentiation culture, Stem Cells, **22**, 275–282 (2004).
8. **Zweigerdt, R., Olmer, R., Singh, H., Haverich, A., and Martin, U.:** Scalable expansion of human pluripotent stem cells in suspension culture, Nat. Protoc., **6**, 689–700 (2011).
9. **Singh, H., Mok, P., Balakrishnan, T., Rahmat, S. N., and Zweigerdt, R.:** Up-scaling single cell-inoculated suspension culture of human embryonic stem cells, Stem Cell Res., **4**, 165–179 (2010).
10. **Kwok, C. K., Ueda, Y., Kadari, A., Günther, K., Ergün, S., Heron, A., Schnitzler, A. C., Rook, M., and Edenhofer, F.:** Scalable stirred suspension culture for the generation of billions of human induced pluripotent stem cells using single-use bioreactors, J. Tissue Eng. Regen. Med., **12**, e1076–e1087 (2018).
11. **Nath, S. C., Tokura, T., Kim, M.-H., and Kino-oka, M.:** Botulinum hemagglutinin-mediated in situ break-up of human induced pluripotent stem cell aggregates for high-density suspension culture, Biotechnol. Bioeng., **115**, 910–920 (2017).

12. **Nath, S. C., Horie, M., Nagamori, E., and Kino-oka, M.:** Size- and time-dependent growth properties of human induced pluripotent stem cells in the culture of single aggregate, J. Biosci. Bioeng., **124**, 469–475 (2017).
13. **Trappmann, B., Gautrot, J. E., Connelly, J. T., Strange, D. G., Li, Y., Oyen, M. L., Cohen Stuart, M. A., Boehm, H., Li, B., Vogel, V., and other 3 authors:** Extracellular-matrix tethering regulates stem-cell fate, Nat. Mater., **11**, 642–649 (2012).
14. **Baker, B. M. and Chen, C. S.:** Deconstructing the third dimension: how 3D culture microenvironments alter cellular cues, J. Cell Sci., **125**, 3015–3024 (2012).
15. **Wozniak, M. A. and Chen, C. S.:** Mechanotransduction in development: a growing role for contractility, Nat. Rev. Mol. Cell Biol., **10**, 34–43 (2009).
16. **Cukierman, E., Pankov, R., Stevens, D. R., and Yamada, K. M.:** Taking cell-matrix adhesions to the third dimension, Science, **294**, 1708–1712 (2001).
17. **Farhadifar, R., Röper, J. C., Aigouy, B., Eaton, S., and Jülicher, F.:** The influence of cell mechanics, cell–cell interactions, and proliferation on epithelial packing, Curr. Biol., **17**, 2095–2104 (2007).
18. **Chen, S. S., Fitzgerald, W., Zimmerberg, J., Kleinman, H. K., and Margolis, L.:** Cell–cell and cell–extracellular matrix interactions regulate embryonic stem cell differentiation, Stem Cells, **25**, 553–561 (2007).
19. **Row, S., Liu, Y., Alimperti, S., Agarwal, S. K., and Andreadis, S. T.:** Cadherin-11 is a novel regulator of extracellular matrix synthesis and tissue mechanics, J. Cell Sci., **129**, 2950–2961 (2016).
20. **Li, L., Bennett, S. A., and Wang, L.:** Role of E-cadherin and other cell adhesion molecules in survival and differentiation of human pluripotent stem cells, Cell Adh. Migr., **6**, 59–70 (2012).
21. **Weber, G. F., Bjerke, M. A., and DeSimone, D. W.:** Integrins and cadherins join forces to form adhesive networks, J. Cell Sci., **124**, 1183–1193 (2011).
22. **Vitillo, L., Baxter, M., Iskender, B., Whiting, P., and Kimber, S. J.:** Integrin-associated focal adhesion kinase protects human embryonic stem cells from apoptosis, detachment, and differentiation, Stem Cell Rep., **7**, 167–176 (2016).
23. **Nakagawa, M., Taniguchi, Y., Senda, S., Takizawa, N., Ichisaka, T., Asano, K., Morizane, A., Doi, D., Takahashi, J., Nishizawa, M., and other 3 authors:** A novel efficient feeder-free culture system for the derivation of human induced pluripotent stem cells, Sci. Rep., **4**, 3594 (2014).
24. **Kim, M.-H., Masuda, E., and Kino-oka, M.:** Kinetic analysis of deviation from the undifferentiated state in colonies of human induced pluripotent stem cells on feeder layers, Biotechnol. Bioeng., **111**, 1128–1138 (2014).
25. **Kim, M.-H. and Kino-oka, M.:** Switching between self-renewal and lineage commitment of human induced pluripotent stem cells via cell–substrate and cell–cell interactions on a dendrimer-immobilized surface, Biomaterials, **35**, 5670–5678 (2014).
26. **Stover, A. E. and Schwartz, P. H.:** Adaptation of human pluripotent stem cells to feeder-free conditions in chemically defined medium with enzymatic single-cell passaging, Methods Mol. Biol., **767**, 137–146 (2011).
27. **Shirayoshi, Y., Okada, T. S., and Takeichi, M.:** The calcium-dependent cell–cell adhesion system regulates inner cell mass formation and cell surface polarization in early mouse development, Cell, **35**, 631–638 (1983).
28. **Suemori, H., Yasuchika, K., Hasegawa, K., Fujioka, T., Tsuneyoshi, N., and Nakatsuji, N.:** Efficient establishment of human embryonic stem cell lines and long-term maintenance with stable karyotype by enzymatic bulk passage, Biochem. Biophys. Res. Commun., **345**, 926–932 (2006).
29. **Beers, J., Gulbranson, D. R., George, N., Siniscalchi, L. I., Jones, J., Thomson, J. A., and Chen, G.:** Passaging and colony expansion of human pluripotent stem cells by enzyme-free dissociation in chemically defined culture conditions, Nat. Protoc., **7**, 2029–2040 (2012).
30. **Bai, H., Chen, K., Gao, Y. X., Arzigian, M., Xie, Y. L., Malcosky, C., Yang, Y. G., Wu, W. S., and Wang, Z. Z.:** Bcl-xL enhances single-cell survival and expansion of human embryonic stem cells without affecting self-renewal, Stem Cell Res., **8**, 26–37 (2012).
31. **Hossini, A. M., Quast, A. S., Plötz, M., Grauel, K., Exner, T., Küchler, J., Stachelscheid, H., Eberle, J., Rabien, A., Makrantonaki, E., and Zouboulis, C. C.:** PI3K/AKT signaling pathway is essential for survival of induced pluripotent stem cells, PLoS One, **11**, e0154770 (2016).